Received: 11 February 2025 | Revised: 24 September 2025 | Accepted: 4 October 2025

DOI: 10.1002/bcp.70333

ORIGINAL ARTICLE

Population pharmacokinetics of TBAJ-587 and its main metabolites—Evaluation of different loading dose strategies and early dose selection

Albin A. M. Leding[1] | Paul Bruinenberg[2] | Almari Conradie[2] | Jerry Nedelman[2] | Antonio Lombardi[2] | Dean Hickman[2] | Ulrika S. H. Simonsson[1]

[1]Department of Pharmaceutical Biosciences, Uppsala University, Uppsala, Sweden

[2]TB Alliance, New York, New York, USA

Correspondence
Ulrika S. H. Simonsson, Department of Pharmaceutical Biosciences, Uppsala University, BMC, Box 591, 75124 Uppsala, Sweden.
Email: ulrika.simonsson@uu.se

Funding information
Innovative Medicines Initiative 2 Joint Undertaking (JU), Grant/Award Number: 853989

Background and Aim: The rise of drug-resistant tuberculosis (TB) poses a need for new drugs and combinations. TBAJ-587, a new diarylquinoline (DARQ), has shown promising efficacy in preclinical studies. This work aimed to describe the pharmacokinetics (PK) of TBAJ-587 and its metabolites M2 and M3 after single ascending dosing in healthy volunteers and to develop a simultaneous population PK model. In addition, to explore different doses in relation to efficacy and safety and to assess the impact of loading doses on exposure levels of TBAJ-587 and its metabolites.

Methods: Pharmacokinetic samples from 42 healthy volunteers following a single dose (25, 50, 100, 200, 400 or 800 mg) were collected for up to Day 126. Population pharmacokinetic modelling was conducted using nonlinear mixed-effects modelling in NONMEM. Simulations from final model were performed to compare against efficacy targets derived from the first-in-class DARQ bedaquiline and safety references based on preclinical studies.

Results and Conclusions: The final model simultaneously described the PK of TBAJ-587, M2 and M3 well. Simulations of final model identified that all simulated doses and regimens resulted in exposures that were below the safety references. A loading dose for 2 weeks resulted in initially higher concentrations, but a limited difference in exposure at 4 weeks and onwards, compared with no loading dose. A 100 mg once daily dose and higher reached the efficacy targets and can be studied further in combinations in phase 2a studies. Name of trial: Evaluation of the Safety, Tolerability, PK of TBAJ-587 in Healthy Adults. Registration number: NCT04890535.

KEYWORDS
metabolite, pharmacometrics, population pharmacokinetics, TBAJ-587, tuberculosis

1 | INTRODUCTION

One challenge in the treatment of tuberculosis (TB) is the emergence of drug resistance (DR-TB).[1] **Bedaquiline**, which is a diarylquinoline (DARQ), an adenosine triphosphate synthase inhibitor, was over a decade ago conditionally approved to be used against DR-TB,[2] now approved, and has also recently been included in novel regimens and studies in multiple different clinical

trials such as Nix-TB, ZeNIX, TB-PRACTECAL and SimpliciTB.[3–6] In the trials, the dosing regimens with bedaquiline all included loading doses of bedaquiline of 2 or 8 weeks, maintenance dose once daily or three times weekly for 9–24 weeks and doses of 100, 200 or 400 mg.[3–6] A loading dose period is needed to reach effective concentrations more quickly due to bedaquiline's very long terminal half-life which is more than 5 months.[7] Label for bedaquiline states that bedaquiline should first be given as 400 mg once daily for 2 weeks followed by 200 mg three times per week for 22 weeks.[8] Since approval, there has been an increase in recorded resistance to bedaquiline. For example, in Mozambique, an increase from 3% to 14% of bedaquiline resistance prevalence was observed between 2016 and 2021.[9] This highlights the need for next-generation DARQs.

TBAJ-587 is a new chemical entity similar to bedaquiline and is also classified as a DARQ. TBAJ-587 has been shown to have a higher potency than bedaquiline against *Mycobacterium tuberculosis* (H37Rv strain) in both replicating and non-replicating in vitro assays.[10] In BALB/c mice experiments, TBAJ-587 has shown superior sterilization activity compared with bedaquiline, both in monotherapy and when TBAJ-587 was substituted in different combinations in both a bedaquiline-susceptible strain (H37Rv)[11,12] and a bedaquiline-resistant mutant strain (Rv0678 mutant).[12] Bedaquiline's *N*-desmethyl metabolite, bedaquiline-M2, has been linked to increasing heart rate corrected time between the left-to-right depolarization of the interventricular septum and ventricular repolarization (QTc prolongation) in patients, highlighting the importance of knowledge of potential metabolites for DARQs.[13] The two human metabolites to TBAJ-587, M2 and M3, share the same molecular weight and are formed by mono-demethylation. The first in class drug bedaquiline is mainly metabolized by cytochrome P450 3A4.[14] It is, however, not known which enzymes that are involved in the metabolism of TBAJ-587. The in vitro bactericidal activity has been studied for M2 and M3 and the minimum inhibitory concentration (MIC) of M2 was ~10-fold larger than TBAJ-587, while the MIC of M3 was similar to TBAJ-587.[15] In BALB/c mice, TBAJ-587 and M3 share with bedaquiline the characteristic of having a long terminal half-life.[11]

Dose selection based on exposure matching has been used within different fields such as paediatric studies[16] and formulation comparison.[17] The approach is to take accessible information and with assumptions of the extrapolation try to match exposure indices of different populations or different formulations. Adaptation of the exposure matching approach gives an opportunity to further explore TBAJ-587 efficacy-based dose selection because it is a second-in-class DARQ.

This work aimed to describe the pharmacokinetics (PK) of TBAJ-587 and its metabolites M2 and M3 after single ascending dosing in healthy volunteers and to develop a simultaneous population PK model. In addition, to explore different doses in relation to efficacy and safety and to assess the impact of loading doses on exposure levels of TBAJ-587 and its metabolites.

What is already known about this subject

- TBAJ-587 is a new antitubercular drug that is a second-in-class diarylquinoline drug with promising preclinical efficacy and safety profile.
- Selecting the dose(s) to be used in early clinical development in patients can be complex.

What this study adds

- The pharmacokinetics of TBAJ-587 and its active metabolites were described using population pharmacokinetic analysis.
- Simulations using efficacy targets derived from the first-in-class diarylquinoline bedaquiline and safety references based on preclinical studies predicted 100 mg once daily dosing with or without a loading period to achieve safe and efficacious exposures.

2 | MATERIALS AND METHODS

2.1 | Subjects and study design

The study was a partially blinded, placebo-controlled, randomized, single ascending dose (SAD) with food effect cohort trial (NCT04890535—Part 1).[18] The trial was approved by the regulatory authority and local ethics committee at the site (approval ID NL73973.056.20), and participants gave written informed consent. The participants were healthy volunteers who were male or female of non-childbearing potential, between 18 and 64 years of age. Furthermore, the body mass index was between 15.5 and 32.0 kg/m^2 with a minimum weight of 50.0 kg.

Participants were recruited in seven different cohorts: six SAD cohorts and one food-effect cohort. Doses for the SAD cohorts were 25, 50, 100, 200, 400 and 800 mg, from which data were available for 6, 4, 5, 8, 4 and 6 participants, respectively, at the time of this analysis. Nine subjects in the food-effect cohort received a high-calorie and high-fat meal together with a single 200 mg oral dose of TBAJ-587. Plasma samples were collected at 0.5, 1, 1.5, 2, 3, 4, 5, 6, 7, 8, 10, 12, 16, 24, 28, 32, 36, 40, 44, 48, 54, 60, 66, 72, 78, 84, 90, 96, 108, 120, 132, 144, 156, 168, 192, 216, 240, 264, 288 and 312 h post dose. Additionally, in 29 out of 42 subjects (69%), samples were available also at Days 21, 28, 42, 56, 70, 84 and 98. In 23 out of these 29 participants (79%), additional samples were available at Days 112 and 126.

TBAJ-578, M2 and M3 plasma concentrations were determined with a validated high-performance liquid chromatography–tandem

mass spectrometry method within the same sample. The linear range of the method was 1–1000 ng/mL for all four analytes. Observations below the lower limit of quantification (LLOQ), that is, 1 ng/mL, were reported as below the quantification limit (BQL). Intra-assay coefficient of variation (CV) and residual error were 1.0% to 12.8% and −9.4% to 12.8%, respectively, for TBAJ-587; 1.8% to 13.2% and −14.5% to 7.4%, respectively, for M2; and 1.8% to 14.0% and −13.0% to 11.3%, respectively, for M3. The inter-assay CV and residual error were 4.0% to 9.9% and −5.1% to 4.8%, respectively, for TBAJ-587; 3.5% to 13.2% and −5.3% to 2.6%, respectively, for M2; and 2.9% to 13.3% and −0.7% to 8.0%, respectively, for M3. A minimum of 6 quality control samples were included in each analysis, and incurred sample reanalysis (ISR) was within the 20% assay variability criterion for 97%, 89% and 95%, of samples for TBAJ-587, M2 and M3, respectively, thereby adhering to the condition of 2/3 of the repeats needing to be within the variability defined by the ICH-M10 guidance.

2.2 | Population pharmacokinetic analysis

Exploratory graphical analysis was performed to identify outliers and indications of non-linearities in the PK profiles of the compounds. Concentration *vs*. time data of TBAJ-587, M2 and M3 were included in this analysis. Modelling was performed on natural-logarithm-transformed molar concentration data.

One-, two- and three-compartmental disposition models with first-order elimination were evaluated for TBAJ-587. Absorption models explored for TBAJ-587 were zero and first order, with or without lag-time or dynamic absorption transit compartments.[19] Different residual error models were tested throughout the model development. Interindividual variability (IIV) was evaluated on all parameters as in Equation (1).

$$P_i = P \times e^{\eta_i}, \tag{1}$$

where P denotes the parameter, η denotes a normally distributed random variable with mean 0 and standard deviation ω and i denotes the individual.

Different methods to handle BQL observations were explored such as ignoring all BQL observations, setting the last BQL observation in the absorption phase and the first BQL observation in the elimination phase to half the LLOQ, and the M3 method.[20,21]

Once the parent PK model was developed, it was fixed and separate sub-models for M2 and M3 were developed, one at a time, assuming parallel formation, using the fixed TBAJ-587 PK model and the assumption of f_m, the fraction of TBAJ-587 cleared to metabolite, equalling one. Different methods to handle BQL observations were explored as described above. Each metabolite was investigated by evaluating one-, two- or three-compartment disposition with first-order elimination. Different residual error models were assessed during the model development procedure. IIV was evaluated in all parameters as in Equation (1).

After each structural PK sub-model was developed, food and dose dependencies were explored on typical parameters using stepwise covariate modelling (SCM)[22] with forward inclusion criteria at a 5% significance level and 1% for backward elimination. Dose was treated as a continuous covariate and evaluated on absorption (k_a and MTT), relative bioavailability (F), metabolite formation ($f_{m,M2}$ and $f_{m,M3}$) and elimination parameters ($CL_{TBAJ-587}$, CL_{M2} and CL_{M3}), using the SCM default expressions for linear, piece-wise linear, exponential and power with the addition of an E_{max} function as in Equation (2):

$$P_{dose} = TVP\frac{MAX_{dose} \times Dose}{D_{50} + Dose}, \tag{2}$$

where P_{dose} is the parameter with covariate effect, TVP is the typical parameter, Dose is the dose in mg, D_{50} is the dose at 50% of the maximal change in the parameter and MAX_{dose} is the maximal effect on the parameter P. Food effect was evaluated as a categorical covariate on absorption (k_a and MTT), relative bioavailability (F) and metabolite formation ($f_{m,M2}$ and $f_{m,M3}$) parameters.

In a final step, the sequentially developed metabolite sub-models were estimated simultaneously with the parent PK model fixed and covariance evaluated between random effects in mean-transit-time (MTT) and relative bioavailability (F), as well as between the parent clearance ($CL_{TBAJ-587}$) and F as indicated by post hoc η correlation graphical analysis, acknowledging shrinkage in these plots.[23]

2.3 | Model selection and evaluation

Models were evaluated based on graphical diagnostics, such as observations *vs*. individual predictions, observations *vs*. population predictions, individual residual errors *vs*. population predictions, individual residual errors *vs*. time and individual plots. Furthermore, visual predictive checks (VPCs),[23,24] relative standard error (RSE) of parameter estimates, objective function value (OFV), scientific plausibility and parsimony were used throughout the model development process. Selection between nested models was based on a decrease in OFV of 3.84 and a 5% significance level for one degree of freedom. Confidence intervals for final parameter estimates were generated using sampling importance resampling (SIR).[25]

2.4 | Prediction of optimal maintenance dose and influence of loading dose in relation to efficacy and safety

The exposure of TBAJ-587 and metabolites after different maintenance and loading doses was simulated using the final PK model and explored in relation to efficacy targets and safety references. There were two safety references based on a 3-month dog toxicity study,[26] each defined by the sum of the AUC_{0-24h}'s of TBAJ-587 and M3, denoted AUC_{sum}: 113.6 h × mg/L, the AUC_{sum} at the no-observed-adverse-effect-level dose of 10 mg/kg, and 185 h × mg/L, the

AUC_{sum} at 20 mg/kg, the dose where cardiotoxicity was noted. The M2 has been reported not to contribute to the cardiotoxicity in a 3-month dog toxicity study[26] and therefore not included in the safety references in this analysis.

Two different efficacy targets were derived based on exposures of bedaquiline after dosing 400 mg daily for 2 weeks followed by 200 mg three times weekly per the label. The first exposure target was derived using bedaquiline average daily concentrations over time accounting for the potency difference between TBAJ-587 and bedaquiline. The median TBAJ-587/bedaquiline MIC ratio was 0.10, which was derived from matching MIC values from 96 different clinical isolates (0.050–0.40; 5th–95th percentiles). TBAJ-587 and bedaquiline are both highly bound (>99.9%), and as such, the exposure matching was done using total concentrations. Efficacy Target 1 was derived as in Equation (3):

$$\text{Efficacy Target 1 concentration}\,(t) = C_{\text{avg,BDQ}}(t) \times \frac{\text{MIC}_{\text{TBAJ-587}}}{\text{MIC}_{\text{BDQ}}}, \quad (3)$$

where $C_{\text{avg,BDQ}}(t)$ is the model-predicted typical daily average concentration of bedaquiline from a previous developed model[27] at a specific time point following previously described simulation set-up,[28] $\text{MIC}_{\text{TBAJ-587}}$ is the MIC of TBAJ-587 and MIC_{BDQ} is the MIC of bedaquiline. Efficacy Target 1 with the 5th–95th MIC distribution was compared with the model-predicted daily average concentration of TBAJ-587.

The second efficacy target was derived using the sum of bedaquiline and the metabolite bedaquiline-M2 daily average concentrations accounting for the potency difference between bedaquiline and TBAJ-587 as well as the potency difference between bedaquiline-M2 and TBAJ-587. The TBAJ-587/bedaquiline-M2 MIC ratio was 0.041 (strain: H37Rv, data on file). The MIC for the metabolite was derived from a separate experiment than the clinical isolates experiment and therefore did not have a distribution. TBAJ-587, bedaquiline and metabolites were assumed to have comparable fractions unbound, and thereby, total concentration was compared. Efficacy Target 2 was derived in Equation (4):

$$\text{Efficacy Target 2 concentration}\,(t) = C_{\text{avg,BDQ}}(t) \times \frac{\text{MIC}_{\text{TBAJ-587}}}{\text{MIC}_{\text{BDQ}}} + C_{\text{avg,BDQ-M2}}(t) \times \frac{\text{MIC}_{\text{TBAJ-587}}}{\text{MIC}_{\text{BDQ-M2}}}, \quad (4)$$

where $C_{\text{avg,BDQ-M2}}(t)$ is the predicted typical daily average concentration of bedaquiline-M2 at time t[27,28] and $\text{MIC}_{\text{BDQ-M2}}$ is the MIC of bedaquiline-M2. Efficacy Target 2 with the 5th–95th MIC distribution was compared with the sum of the daily average concentration of TBAJ-587 and the potency-adjusted daily average concentration of M3.

Concentration-*vs.*-time profiles of TBAJ-587, M2 and M3 were simulated with the final population PK model with food effect. Different 2-week loading doses, scaled from the maintenance dose (25, 50, 100 or 200 mg daily), followed by 10 weeks of daily maintenance doses were simulated and compared with scenarios without loading dose. The ratios explored of loading dose to maintenance dose were 2:1, 3:1 and 4:1. AUC_{0-24h} for the different scenarios was predicted using the final population PK model and the daily average concentration (C_{avg}) was calculated given Equation (5):

$$C_{\text{avg}} = \frac{\text{AUC}_{0-24\text{h}}}{24}. \quad (5)$$

The predicted C_{avg} was compared with the efficacy targets and the predicted AUC_{0-24h} was compared with the safety references for the different maintenance doses and loading doses. Daily doses were simulated to reduce fluctuation and generate a practical regimen.

2.5 | Software

The population PK data were analysed with NONMEM (Version 7.4.3)[29] using first-order conditional estimation (FOCE)[30] on an Intel Xeon V4 CPU-based cluster running with parallelization on Scientific Linux (Version 7.9.2009) with GCC (Version 8.3.0)[31] as compiler. Pearl-speaks-NONMEM (Version 5.0.0)[32] was utilized to control NONMEM, execute SCM[22] and SIR[25] and create VPCs.[23,24] Plots and simulations were generated using R (Version 4.1.2) with RStudio (Version 2021.09.2+382).[33] The R packages used for model evaluations and simulations were tidyverse (Version 1.3.1),[34] deSolve (Version 1.33)[35] and xpose4 (Version 4.7.1).[36,37]

2.6 | Nomenclature of targets and ligands

Key protein targets and ligands in this article are hyperlinked to corresponding entries in http://www.guidetopharmacology.org and are permanently archived in the Concise Guide to PHARMACOLOGY 2023/24.[38]

3 | RESULTS

3.1 | Data

The data included in the analysis were from 42 subjects with 1929 observations for each compound, that is, TBAJ-587, M2 and M3, collected up to Day 126. For TBAJ-587, M2 and M3, BQL observations comprised 2%, 46% and 28%, respectively. Individual concentration *vs.* time profiles by dose are shown in Figure 1. Abundance in plasma was in decreasing order: TBAJ-587, M3 and M2.

The M3 method was not explored during the TBAJ-587 PK submodel development due to the low proportion of BQL. Setting the first TBAJ-587 BQL and last BQL observations in the decreasing and ascending PK curve to LLOQ/2 generated higher RSE compared with omitting all TBAJ-587 BQL data, wherefore the BQL data were omitted. The M3 method generated unstable models for both M2 and M3

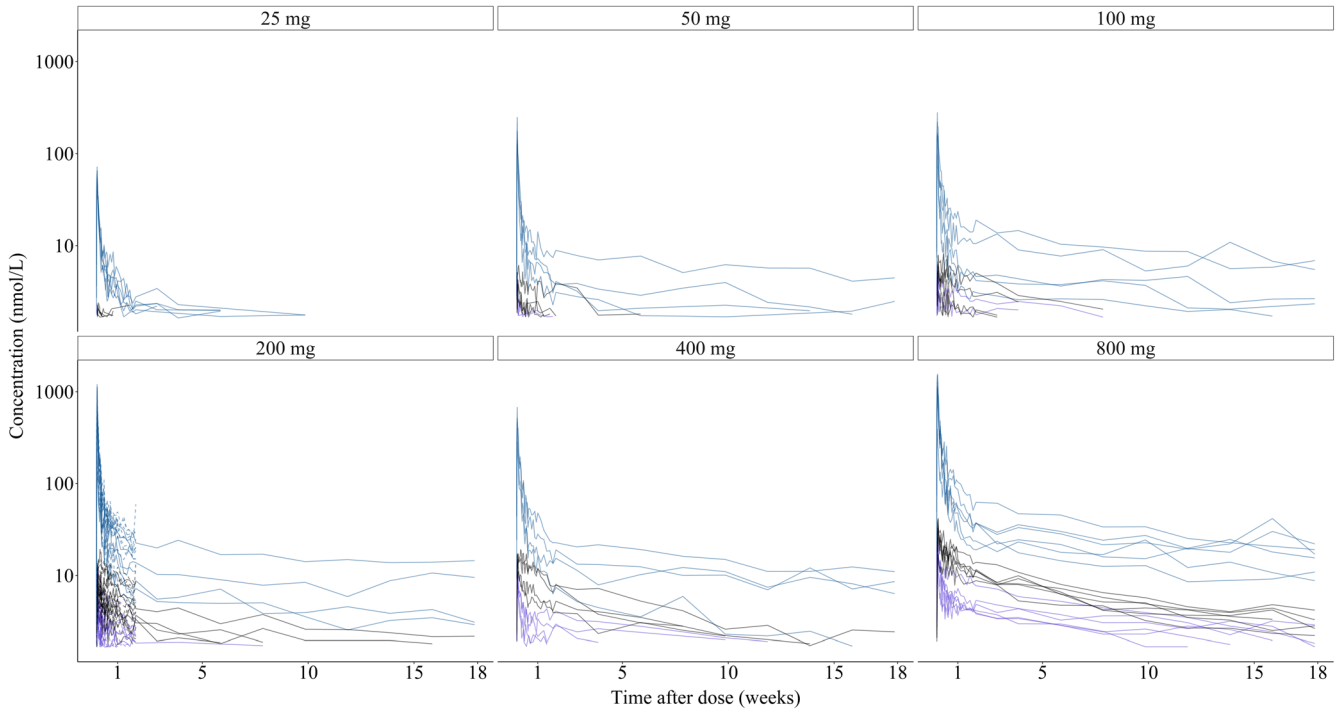

FIGURE 1 Individual concentrations *vs.* time of TBAJ-587 (blue), M2 (purple) and M3 (black) after different oral doses of TBAJ-587 with food (dashed line) or fasted (solid line), stratified on dose.

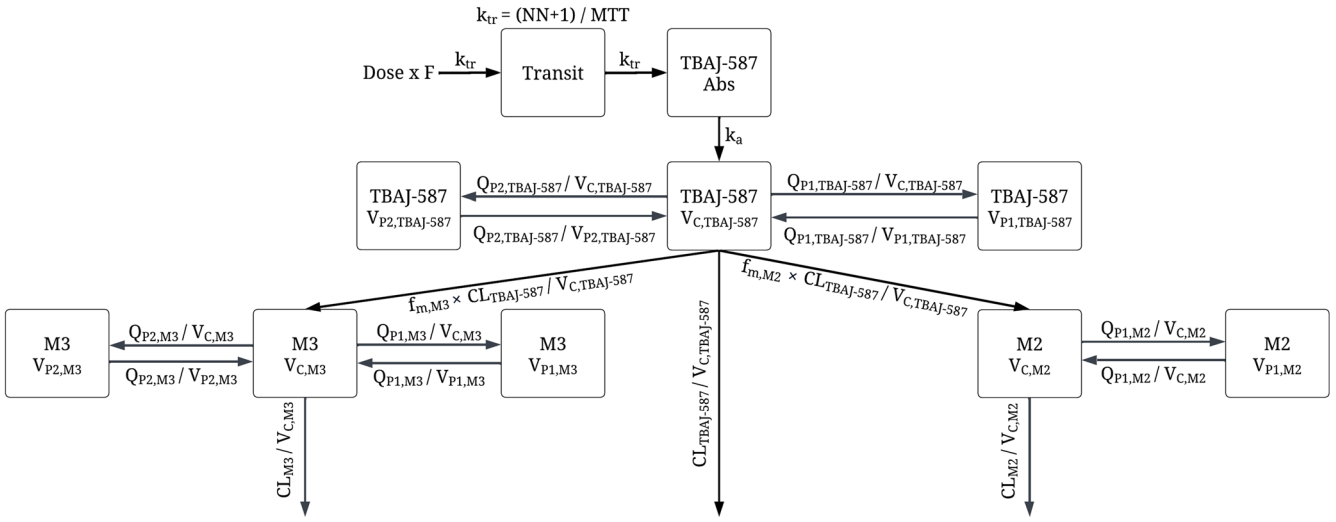

FIGURE 2 Structural overview of the final population pharmacokinetic model describing TBAJ-587, M2 and M3. *F*, relative bioavailability; k_{tr}, transit rate constant; NN, number of transit compartment; MTT, mean transit time; Abs, absorption compartment; k_a, absorption rate; $V_{C,TBAJ-587}$, TBAJ-587 central distribution volume; $V_{P1,TBAJ-587}$, first TBAJ-587 peripheral distribution volume; $V_{P2,TBAJ-587}$, second TBAJ-587 peripheral distribution volume; $Q_{P2,TBAJ-587}$, TBAJ-587 inter-compartmental clearance from $V_{C,TBAJ-587}$ to $V_{P2,TBAJ-587}$; $Q_{P1,TBAJ-587}$, TBAJ-587 inter-compartmental clearance from $V_{C,TBAJ-587}$ to $V_{P1,TBAJ-587}$; $CL_{TBAJ-587}$, TBAJ-587 clearance; $f_{m,M3}$, M3 relative fraction metabolized; $f_{m,M2}$, M2 relative fraction metabolized; $V_{C,M3}$, M3 central distribution volume; $V_{P1,M3}$, first M3 peripheral distribution volume; $V_{P2,M3}$, second M3 peripheral distribution volume; $Q_{P2,M3}$, M3 inter-compartmental clearance from $V_{C,M3}$ to $V_{P2,M3}$; $Q_{P1,M3}$, M3 inter-compartmental clearance from $V_{C,M3}$ to $V_{P1,M3}$; CLM3, M3 clearance; $V_{C,M2}$, M2 central distribution volume; $V_{P1,M2}$, first M2 peripheral distribution volume; $Q_{P1,M2}$, M2 inter-compartmental clearance from $V_{C,M2}$ to $V_{P1,M2}$; CL_{M2}, M2 clearance.

metabolite sub-models. Instead, M2 and M3 BQL data were omitted except for the first and last BQL observations in the decreasing and ascending PK curve, respectively, which were set to LLOQ/2 (0.5 ng/mL).

3.2 | Population pharmacokinetic modelling

Because no data were available under intravenous dosing, all clearance and volume parameters should be interpreted as apparent oral

TABLE 1 Parameter estimates of the final population model of TBAJ-587, M2 and M3.

	Typical estimate			IIV		
Parameter[a]	Estimate	RSE (%)	CI (2.5–97.5%)[b]	CV (%)[c]	RSE (%)	CI (2.5–97.5%)[b]
TBAJ-587 sub-model						
F^{fasted}	1 FIX			41.9	12.0	34.3–53.2
k_a (h^{-1})	0.0866	3.5	0.0818–0.930	19.0	11.8	14.7–23.1
$CL_{TBAJ-587}$ (L/h)	5.40	8.4	4.70–6.24	42.2	28.1	28.6–63.2
$V_{C,TBAJ-587}$ (L)	88.2	6.8	76.7–100	48.2	13.9	35.3–65.3
$Q_{P1,TBAJ-587}$ (L/h)	31.1	6.4	28.9–33.7			
$V_{P1,TBAJ-587}$ (L)	1910	8.7	1640–2180	38.5	17.2	28.1–52.0
$Q_{P2,TBAJ-587}$ (L/h)	31.5	4.0	29.2–33.5			
$V_{P2,TBAJ-587}$ (L)	22 500	3.9	20 700–24 900	34.3	14.5	25.1–44.5
MTT^{fasted} (h)	0.837	4.5	0.763–0.912	37.1	13.2	29.0–46.0
NN	2.36	8	2.14–2.64			
Fed state on F^{fasted}[d]	0.688	18.6	0.392–0.965			
Dose covariate on $CL_{TBAJ-587}$[e]	0.298	28.8	0.144–0.466			
Dose covariate on k_a[f]	−0.00046	32.0	−0.000669 to −0.000277			
Fed state on MTT^{fasted}[d]	0.958	14.0	0.643–1.29			
Additive residual error on logarithmic scale	0.0337	5.0	0.0315–0.0363			
M2 and M3 sub-models						
$f_{m,M2}$	1 FIX			12.5	15.2	9.15–16.8
CL_{M2} (L/h)	34.1	6.1	30.9–37.5			
$V_{C,M2}$ (L)	247	8.5	216–288	60.5	12.9	46.5–78.4
$V_{P1,M2}$ (L)	12 200	6.5	10 800–13 700	49.5	11.2	38.7–61.4
$Q_{P1,M2}$ (L/h)	174	5.0	131–189			
$f_{m,M3}$	1 FIX					
CL_{M3} (L/h)	18.5	7.8	16.7–20.6	22.3	30.0	12.9–32.8
$V_{C,M3}$ (L)	816	6.0	739–906	31.5	18.1	23.5–43.1
$V_{P1,M3}$ (L)	1630	22.1	1170–2330			
$Q_{P1,M3}$ (L/h)	9.09	17.9	5.97–11.8			
$V_{P2,M3}$ (L)	3010	6.5	2740–3340			
$Q_{P2,M3}$ (L)	99.6	6.4	90.9–108			
Dose covariate on $f_{m,M2}$[e]	−0.373	16.5	−0.451 to −0.294			
Fed state on $f_{m,M2}$[d]	−0.547	20.8	−0.657 to −0.0424			
Dose covariate on CL_{M2}[e]	0.146	31.2	0.0666–0.217			
Dose covariate on $f_{m,M3}$[e]	−0.418	14.3	−0.489 to −0.346			
Fed state on $f_{m,M3}$[d]	−0.479	24.8	−0.595 to −0.341			
M2 additive residual error on logarithmic scale	0.0267	8.3	0.0246–0.0293			
M3 additive residual error on logarithmic scale	0.0382	6.6	0.0356–0.0412			

Abbreviations: CL_{M2}, M2 clearance; CL_{M3}, M3 clearance; $CL_{TBAJ-587}$, TBAJ-587 clearance; F^{fasted}, relative bioavailability in fasted condition; $f_{m,M2}$, relative fraction metabolized to M2; $f_{m,M3}$, relative fraction metabolized to M3; k_a, absorption rate; MTT, mean transit time; NN, number of transit compartment; $Q_{P1,M2}$, M2 inter-compartmental clearance to $V_{P1,M2}$ compartment; $Q_{P1,M3}$, M3 inter-compartmental clearance to $V_{P1,M3}$ compartment; $Q_{P1,TBAJ-587}$, TBAJ-587 inter-compartmental clearance to $V_{P1,TBAJ-587}$ compartment; $Q_{P2,M3}$, M3 inter-compartmental clearance to $V_{P2,M3}$ compartment; $Q_{P2,TBAJ-587}$, TBAJ-587 inter-compartmental clearance to $V_{P2,TBAJ-587}$ compartment; $V_{C,M2}$, M2 central distribution volume; $V_{C,M3}$, M3 central distribution volume; $V_{C,TBAJ-587}$, TBAJ-587 central distribution volume; $V_{P1,M2}$, M2 first peripheral distribution volume; $V_{P1,M3}$, M3 first peripheral distribution volume; $V_{P1,TBAJ-587}$, TBAJ-587 first peripheral distribution volume TBAJ-587; $V_{P2,M3}$, M3 second peripheral distribution volume; $V_{P2,TBAJ-587}$, TBAJ-587 second peripheral distribution volume.

[a]Because no data were available under intravenous dosing, all clearance and volume parameters should be interpreted as apparent oral parameter estimates. For metabolites, clearances and volumes are additionally relative to unknown fractions metabolized.

[b]CI = confidence interval derived using sampling/importance resampling (SIR) methodology.

[c]CV = coefficient of variation derived as $CV = \sqrt{e^{\omega^2} - 1} \times 100\%$.

[d]Imputation described as $P_{Fed} = P_{Fasted}(1 + Covariate_{Fed})$; P is the parameter of interest.
[e]Power relationship described as $P_{Dose} = P_{200\,mg}\frac{Dose}{Dose_{200\,mg}}^{Covariate_{Dose}}$; P is the parameter of interest.
[f]Exponential relationship described as $P_{Dose} = P_{200\,mg}e^{Covariate_{Dose}\times(Dose-Dose_{200\,mg})}$; P is the parameter of interest.

values. For metabolites, clearances and volumes are additionally relative to unknown fractions metabolized.

The final TBAJ-587 PK sub-model described the data well and consisted of a three-compartment disposition model with first-order elimination (Figures 2 and S1), which had an OFV drop of 733 points compared with a two-compartment model. The estimated TBAJ-587 oral clearance ($CL_{TBAJ-587}$) in the fasted state at a dose of 200 mg was 5.40 L/h, and the central volume of distribution ($V_{C,TBAJ-587}$) was 88.2 L. A statistically significant ($p < 0.01$) non-linear dose-dependent relationship (power), where $CL_{TBAJ-587}$ increased with increasing doses, was included in the final TBAJ-587 sub-model. The estimated absorption rate (k_a) was 0.0866 h^{-1} at a dose of 200 mg, and a nonlinear relationship with dose was found to be statistically significant ($p < 0.01$), resulting in k_a ranging between 0.0939 and 0.0657 h^{-1} for doses of 25–800 mg. The delay in absorption was best described with absorption transit compartments, which provided a drop in OFV of 610 points, compared with a model with lag time. Mean absorption transit time was estimated to be 0.837 h without food and was twice as high in the presence of food while relative bioavailability increased by 68.8% in the presence of food ($p < 0.01$). The terminal half-life was predicted to range from 3.5 to 9.0 months for the explored dose range in the dataset as identified using simulations with the final model. The highest IIV was estimated for $V_{C,TBAJ-587}$ (48.2%) and $CL_{TBAJ-587}$ (42.2%) (Table 1). Residual variability was modelled with an additive error on a logarithmic scale. VPCs confirmed that the final sub-model adequately captured the data (Figure S1).

M3 was best described by a three-compartmental disposition model with first-order elimination (Figures 2 and S3), which had an OFV drop of 17 points compared with a two-compartment model. The estimated M3 clearance (CL_{M3}) was 18.5 L/h, and the central volume of distribution of M3 ($V_{C,M3}$) was estimated as 816 L (Table 1). The relative fraction metabolized to M3 decreased in a power-law relationship with increasing doses ($p < 0.01$), and it was 47.1% lower in the presence of food compared with without food ($p < 0.01$). The terminal half-life of M3 was predicted to be in a similar range as TBAJ-587. IIV in CL_{M3} was estimated to be 22.3% and 31.5% for the $V_{C,M3}$. A separate residual variability for M3 was estimated with an additive error on the logarithmic scale.

The M2 metabolite was best described by a two-compartment disposition model with first-order elimination (Figures 2 and S2), which had an OFV drop of 2640 points compared with a one-compartment model. The estimated M2 clearance at a dose of 200 mg (CL_{M2}) was 34.1 L/h, and the central volume of distribution of M2 ($V_{C,M2}$) was estimated to be 247 L (Table 1). The relative fraction metabolized to M2 decreased in a power-law relationship with increasing doses ($p < 0.01$), and it was 54.7% lower in the presence of food ($p < 0.01$). CL_{M2} increased non-linearly with increasing doses ($p < 0.01$). The terminal half-life of M2 was predicted to be in a similar range as TBAJ-587. IIV was estimated in $V_{C,M2}$ (60.5%), peripheral volume of distribution ($V_{P1,M2}$) (49.5%) and the relative fraction metabolized to M2 (12.5%). Residual variability was explained independently from TBAJ-587 and M3 with an additive error model on the logarithmic scale.

The simultaneous fit of all three sub-models provided similar parameter estimates but higher uncertainties in the model parameter estimates compared with the estimates from the individual metabolite sub-models using a fixed parent sub-model and was therefore not selected as the final model. Parameter estimates for the simultaneous fit are provided in Table S1. The final NONMEM code can be found in Code S1. The VPCs of the final model, Figures S2–S4, show that the final model described the compounds well, and Figure S5 shows that the assumption of BQL data handling performed well in predicting the percentages BQL.

Table S2 displays predicted AUC_{0-24h} of TBAJ-587, M2 and M3 after 4 weeks of dosing 25–800 mg daily. Increases in predicted exposure were approximately dose-proportional for TBAJ-587, slightly less so for M2 and M3.

3.3 | Prediction of optimal maintenance dose and influence of loading dose in relation to efficacy and safety

Model-predicted C_{avg} of TBAJ-587 over time after different maintenance doses, without loading doses, are shown in Figure 3. As a result of the long half-life, steady state was not reached after 12 weeks of dosing. Loading doses of 2×, 3× and 4× the maintenance dose for 2 weeks were also explored in the simulations, which resulted in initially higher concentrations but did still not result in steady state being reached at 12 weeks. At 4 weeks, the exposure was similar between no loading doses and loading doses. The lowest dosing regimen without a loading dose that reached both efficacy targets over an entire simulated 12-week dosing period was 100 mg once daily (Figures 3 and 4).

The model-predicted AUC_{sum} *vs.* time was used to explore different maintenance doses and loading doses in relation to safety references. Simulations showed that all maintenance doses resulted in exposures lower than the safety references (Figure 5).

4 | DISCUSSION

The selection of efficacy targets by matching bedaquiline exposures with potency correction was possible as the mechanism of action of TBAJ-587 is the same as for bedaquiline. A distribution of MICs from different clinical isolates was used to create a 90% prediction interval for the efficacy target. However, the MIC has the inherent drawback of low resolution because of the two-fold dilutions that are standard

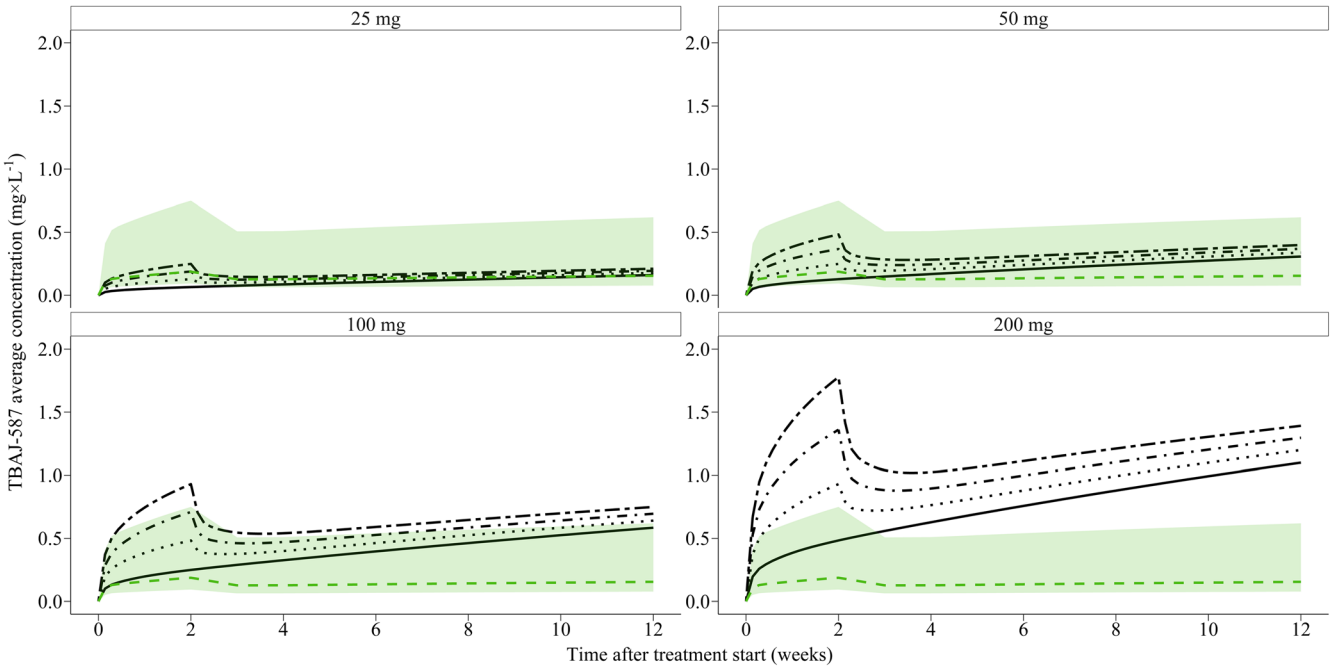

FIGURE 3 Predicted exposure in relation to Efficacy Target 1. Predicted average concentration of TBAJ-587 over time, without (solid line) and with different once daily loading doses for 2 weeks stratified on different once daily maintenance doses (dotted 2 × maintenance, dot-dashed 3 × maintenance and short-long-dashed lines 4 × maintenance). The dashed green line indicates Efficacy Target 1, and the green shaded area represents the 5th and 95th percentile of Efficacy Target 1.

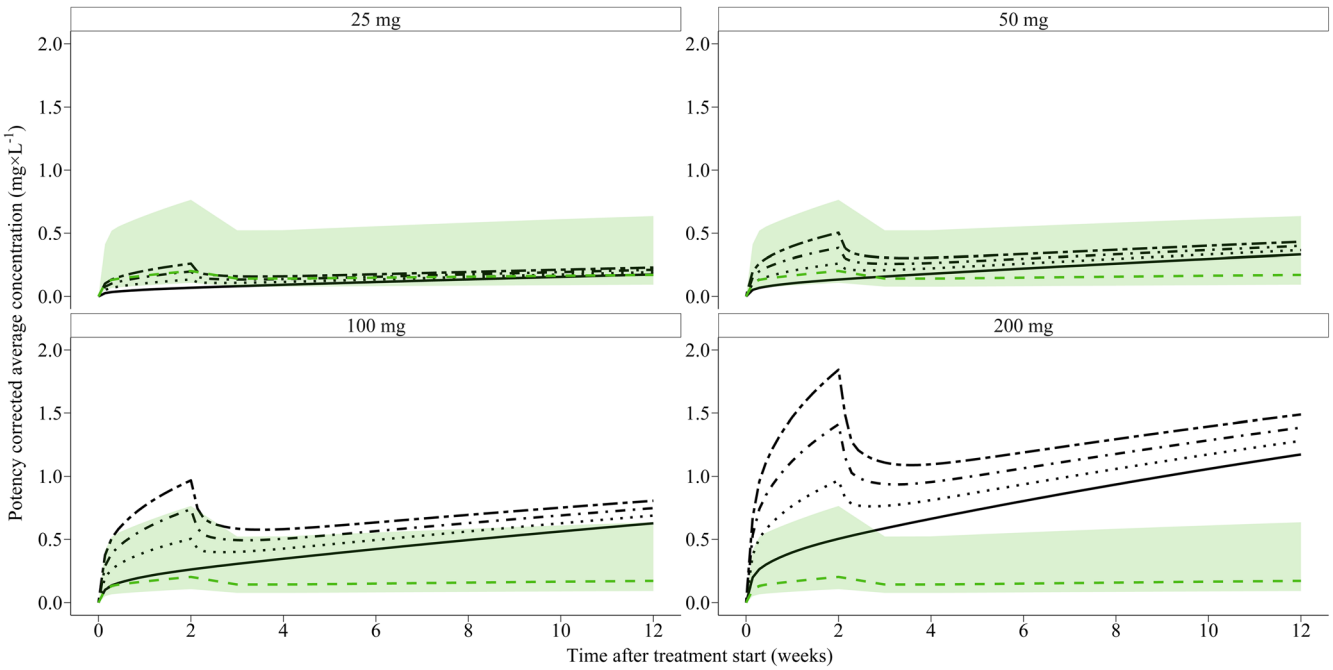

FIGURE 4 Predicted exposure in relation to Efficacy Target 2. Predicted average concentration (C_{avg}) of TBAJ-587 + M3 over time, adjusted for the difference in potency ($C_{avg,TBAJ\text{-}587} \times \frac{MIC_{TBAJ\text{-}587}}{MIC_{TBAJ\text{-}587}} + C_{avg,M3} \times \frac{MIC_{TBAJ\text{-}587}}{MIC_{M3}}$) without (solid line) or with different once daily loading doses (dotted 2 × maintenance, dot-dashed 3 × maintenance and short-long-dashed lines 4 × maintenance), stratified on different once daily maintenance doses. The dashed green line indicates Efficacy Target 2 and the green shaded area represents the 5th and 95th percentile of Efficacy Target 2. The MIC ratio of TBAJ-587/M3 was 0.5 (strain: H37Rv, data on file). The TBAJ-587 metabolite M2 was assumed to not contribute to the efficacy.

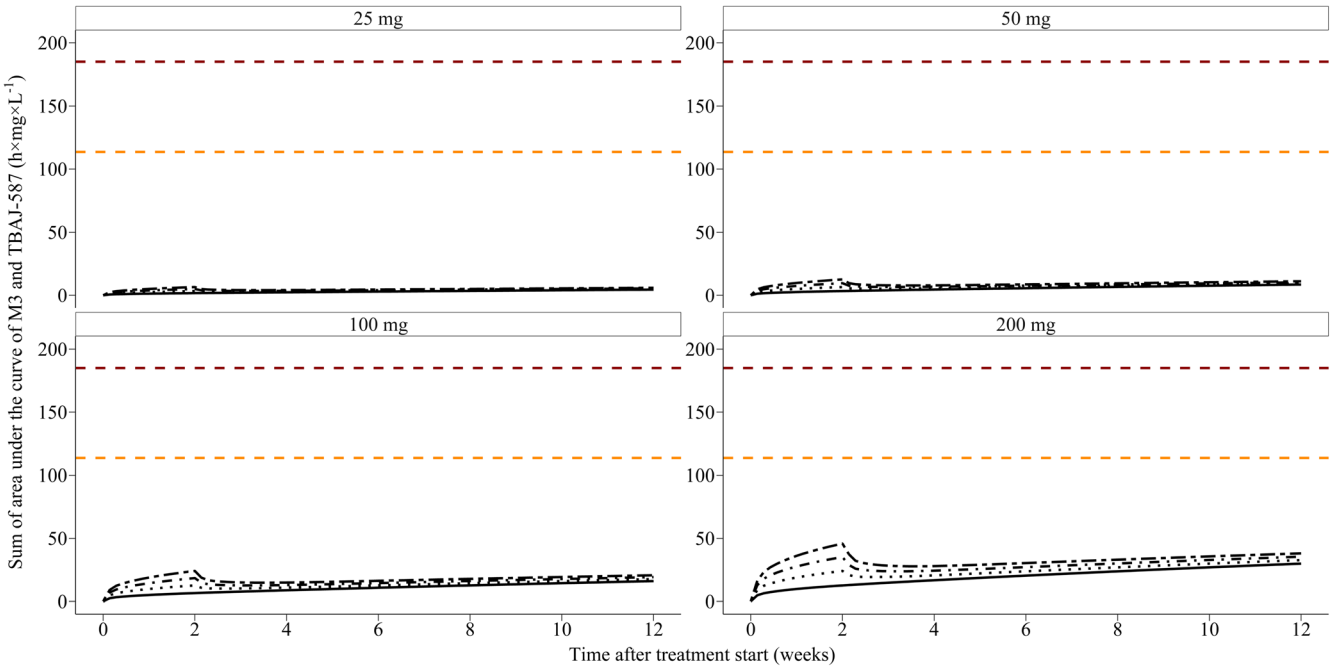

FIGURE 5 Predicted exposure in relation to safety references. Predicted sum of area under the concentration *vs.* time curves (AUC_{sum}) for each day of TBAJ-587 and M3 without (solid line) or with different once daily loading doses (dotted 2 × maintenance, dot-dashed 3 × maintenance and short-long-dashed lines 4 × maintenance), stratified on different doses of once daily maintenance doses. The horizontal dashed red and orange lines indicate the safety references derived from the corresponding AUC_{sum} found in a 3-month dog toxicity study at the exposure where cardiotoxicity was observed and exposure of no-observed-adverse-effect level, respectively.

for MIC determination and lack of time dependency because MIC is a single timepoint measurement. Furthermore, from a single MIC value and from different laboratories, the establishment of between-strain susceptibility is not possible.[39] In future work, preclinical in vitro PKPD data will inform dose selection in a translational context taking into regard site-of-action and other translational factors. Nonetheless, the exposure-matching approach creates a foundation for early dose selection for phase 2a studies of bactericidal activity, based on only nonclinical information (MIC) and data from a SAD study.

In this work, the simulations were done up to 12 weeks, which is a shorter treatment period than the 24 weeks approved for bedaquiline. The reason for targeting a shorter treatment period for TBAJ-587 is the shorter time to sterilization of TBAJ-587 in combinations in mice compared with bedaquiline,[11] which is hypothesized to lead to regimens with shorter treatment duration.

The TBAJ-587 metabolite M3 has been reported to be the microbiologically active metabolite.[15] In this SAD study, it was confirmed that M3 also is the main metabolite of TBAJ-587 in humans. It is not known if M3 from TBAJ-587 causes any QTc prolongation as bedaquiline-M2 does.

Safety references from the 3-month dog toxicity study were used to explore if the predicted doses reaching the efficacy targets could be considered safe. Uncertainties related to the translation from dogs to humans are present because the ratio of M3 formed from TBAJ-587 is higher in dogs than in humans (internal data). For the simulations of exposure in relation to the safety references, the TBAJ-587 and M3 metabolite were assumed to contribute equally to the safety via the AUC_{sum}. Mass-based exposures (mg/L) were summed for convenience rather than molar concentrations because the difference in molecular weight between TBAJ-587 and M3 is only 2%. Future clinical studies in TB patients need to collect safety data from short- and long-term treatment. In addition, tolerability was not considered in the dose predictions and should be monitored also in future phase 2 studies in patients.

The PK after different dose regimens were simulated under fed conditions because it is anticipated that TBAJ-587, like bedaquiline, will be recommended for administration with food. However, only one dose level was administered under fed conditions in the modelled data. Therefore, the predicted exposures assume that the dose dependence of apparent oral clearance, driven by the six dose levels administered under fasting conditions, also applies under fed conditions. Furthermore, the dose dependence on apparent oral clearance in this model results in increasing clearance with increasing dose. Omission or replacement with dose-dependent relative bioavailability decreased the model's performance. The mechanism of the dose non-linearity is not known but describes likely multiple different processes.

The predicted typical half-life of TBAJ-587 ranged from 3.5 to 9.0 months within the dosage range explored in the single-dose data; however, in this study, the PK was followed for 18 weeks after a single dose. Future multiple-dose PK data will potentially refine the predicted half-life. The long half-life of TBAJ-587 suggests the potential need for a regimen that includes a loading dose to quickly achieve effective concentrations. However, simulations showed that loading doses of 2×, 3× and 4× the maintenance dose for 2 weeks resulted

in initially higher concentrations but did still not result in steady state being reached at 12 weeks. At 4 weeks, the exposure was similar between no loading doses and loading doses. The inclusion of a loading dose period might also be considered a more complicated regimen which could increase adherence issues, although a loading dose period of 2 weeks is being used for bedaquiline.

Bedaquiline PK has previously been reported by McLeay et al.[40] to be different among healthy volunteers, DS-TB and MDR-TB patients. TBAJ-587 PK may similarly differ. Whether such a possible difference is large enough to result in different dose/regimen recommendations remains to be studied.

In conclusion, this work presents the PK data in healthy volunteers of TBAJ-587 and its metabolites M2 and M3 after a single dose followed up to Day 126 within the dose range of 25–800 mg. The population PK model developed simultaneously described the PK profiles of TBAJ-587, M2 and M3. Furthermore, the method of early dose recommendation from SAD data and sparse preclinical information was applied for a second-in-class drug. With the early dose recommendation approach, simulations using efficacy targets and safety references identified that doses in the range 25–200 mg daily are safe and a 100 mg daily regimen, with or without loading doses, reaches efficacy targets and can be studied further in combinations in phase 2a studies.

AUTHOR CONTRIBUTIONS

Conceptualization: Albin A. M. Leding, Paul Bruinenberg, Almari Conradie, Jerry Nedelman, Antonio Lombardi, Dean Hickman and Ulrika S. H. Simonsson. *Methodology*: Albin A. M. Leding, Paul Bruinenberg, Almari Conradie, Jerry Nedelman, Antonio Lombardi, Dean Hickman and Ulrika S. H. Simonsson. *Software*: Albin A. M. Leding and Ulrika S. H. Simonsson. *Validation*: Albin A. M. Leding, Paul Bruinenberg, Almari Conradie, Jerry Nedelman, Antonio Lombardi, Dean Hickman and Ulrika S. H. Simonsson. *Formal analysis*: Albin A. M. Leding and Ulrika S. H. Simonsson. *Investigation*: Paul Bruinenberg, Almari Conradie, Jerry Nedelman, Antonio Lombardi and Dean Hickman. *Resources*: Jerry Nedelman and Ulrika S. H. Simonsson. *Data curation*: Albin A. M. Leding, Jerry Nedelman and Ulrika S. H. Simonsson. *Writing—original draft preparation*: Albin A. M. Leding. *Writing—review and editing*: Albin A. M. Leding, Paul Bruinenberg, Almari Conradie, Jerry Nedelman, Antonio Lombardi, Dean Hickman and Ulrika S. H. Simonsson. *Visualization*: Albin A. M. Leding. *Supervision*: Ulrika S. H. Simonsson. All authors have read and agreed to the published version of the manuscript.

ACKNOWLEDGEMENTS

The project leading to this publication has received funding from the Innovative Medicines Initiative 2 Joint Undertaking (JU) under Grant 853989. The JU receives support from the European Union's Horizon 2020 Research and Innovation Programme, EFPIA, Global Alliance for TB Drug Development Non-Profit Organization, Bill & Melinda Gates Foundation and University of Dundee. Link to the website: http://www.imi.europa.eu. This work reflects only the author's views, and the JU is not responsible for any use that may be made of the information it contains. The computations were enabled by resources in projects NAISS 2023/5-492 and NAISS 2023/23-591 provided by the National Academic Infrastructure for Supercomputing in Sweden (NAISS) at UPPMAX, funded by the Swedish Research Council through Grant 2022-06725.

CONFLICT OF INTEREST STATEMENT

TB Alliance has ownership over TBAJ-587.

DATA AVAILABILITY STATEMENT

The data that support the findings of this study are available from TB Alliance but restrictions apply to the availability of these data, which were used under licence for the current study, and so are not publicly available. Data are however available from the authors upon reasonable request and with permission of TB Alliance.

ORCID

Ulrika S. H. Simonsson https://orcid.org/0000-0002-3424-9686

REFERENCES

1. World Health Organization. *Global Tuberculosis Report 2023*. World Health Organization; 2023.
2. Mahajan R. Bedaquiline: first FDA-approved tuberculosis drug in 40 years. *Int J Appl Basic Med Res*. 2013;3(1):1-2. doi:10.4103/2229-516X.112228
3. Conradie F, Diacon AH, Ngubane N, et al. Treatment of highly drug-resistant pulmonary tuberculosis. *N Engl J Med*. 2020;382(10):893-902. doi:10.1056/NEJMoa1901814
4. Conradie F, Bagdasaryan TR, Borisov S, et al. Bedaquiline-pretomanid-linezolid regimens for drug-resistant tuberculosis. *N Engl J Med*. 2022;387(9):810-823.
5. Nyang'wa BT, Berry C, Kazounis E, et al. A 24-week, all-oral regimen for rifampin-resistant tuberculosis. *N Engl J Med*. 2022;387(25):2331-2343.
6. Global Alliance for TB Drug Development. Trial to evaluate the efficacy, safety, and tolerability of BPaMZ in drug-sensitive (DS-TB) adult patients and drug-resistant (DR-TB) adult patients. 2017. https://clinicaltrials.gov/study/NCT03338621
7. van Heeswijk RPG, Dannemann B, Hoetelmans RMW. Bedaquiline: a review of human pharmacokinetics and drug–drug interactions. *J Antimicrob Chemother*. 2014;69(9):2310-2318. doi:10.1093/jac/dku171
8. Janssen Therapeutics. SIRTURO (bedaquiline) tablets, for oral use. Report No. 5631621. 2025. https://www.accessdata.fda.gov/drugsatfda_docs/label/2025/204384s020lbl.pdf
9. Barilar I, Fernando T, Utpatel C, et al. Emergence of bedaquiline-resistant tuberculosis and of multidrug-resistant and extensively drug-resistant *Mycobacterium tuberculosis* strains with *rpoB* Ile491Phe mutation not detected by Xpert MTB/RIF in Mozambique: a retrospective observational study. *Lancet Infect Dis*. 2024;24(3):297-307. doi:10.1016/S1473-3099(23)00498-X
10. Sutherland HS, Tong AST, Choi PJ, et al. 3,5-Dialkoxypyridine analogues of bedaquiline are potent antituberculosis agents with minimal inhibition of the hERG channel. *Bioorg Med Chem*. 2019;27(7):1292-1307. doi:10.1016/j.bmc.2019.02.026
11. Li SY, Converse PJ, Betoudji F, et al. Next-generation diarylquinolines improve sterilizing activity of regimens with pretomanid and the novel oxazolidinone TBI-223 in a mouse tuberculosis model. *Antimicrob Agents Chemother*. 2023;67(4):e00035-23. doi:10.1128/aac.00035-23

12. Xu J, Converse PJ, Upton AM, Mdluli K, Fotouhi N, Nuermberger EL. Comparative efficacy of the novel diarylquinoline TBAJ-587 and bedaquiline against a resistant Rv0678 mutant in a mouse model of tuberculosis. *Antimicrob Agents Chemother*. 2021;65(4):e02418-e02420.
13. Chilukuri DM, Colangelo PM. *Application Number: 204384orig1s000. Report No. 3228191*. Center for Drug Evaluation and Research; 2012. https://www.accessdata.fda.gov/drugsatfda_docs/nda/2012/204384Orig1s000ClinPharmR.pdf
14. Liu K, Li F, Lu J, et al. Bedaquiline metabolism: enzymes and novel metabolites. *Drug Metab Dispos*. 2014;42(5):863-866. doi:10.1124/dmd.113.056119
15. Aguilar Ayala D, Eveque M, Rabodoarivelo M, et al. In vitro killing dynamics of the diarylquinolone TBAJ-587 and its main metabolites against *Mycobacterium tuberculosis*. In: *EMBO Workshop on Tuberculosis 2022*. European Molecular Biology Organization (EMBO); 2022. https://araid.es/en/content/vitro-killing-dynamics-diarylquinolone-tbaj-587-and-its-main-metabolites-against
16. Mulugeta Y, Barrett JS, Nelson R, et al. Exposure matching for extrapolation of efficacy in pediatric drug development. *J Clin Pharmacol*. 2016;56(11):1326-1334. doi:10.1002/jcph.744
17. Samtani MN, Nandy P, Ravenstijn P, et al. Prospective dose selection and acceleration of paliperidone palmitate 3-month formulation development using a pharmacometric bridging strategy. *Br J Clin Pharmacol*. 2016;82(5):1364-1370. doi:10.1111/bcp.13050
18. Global Alliance for TB Drug Development. Evaluation of the safety, tolerability, and pharmacokinetics of TBAJ-587 in healthy adults. 2021. https://clinicaltrials.gov/study/NCT04890535
19. Savic RM, Jonker DM, Kerbusch T, Karlsson MO. Implementation of a transit compartment model for describing drug absorption in pharmacokinetic studies. *J Pharmacokinet Pharmacodyn*. 2007;34(5):711-726. doi:10.1007/s10928-007-9066-0
20. Beal SL. Ways to fit a PK model with some data below the quantification limit. *J Pharmacokinet Pharmacodyn*. 2001;28(5):481-504. doi:10.1023/A:1012299115260
21. Bergstrand M, Karlsson MO. Handling data below the limit of quantification in mixed effect models. *AAPS J*. 2009;11(2):371-380. doi:10.1208/s12248-009-9112-5
22. Jonsson EN, Karlsson MO. Automated covariate model building within NONMEM. *Pharm Res*. 1998;15(9):1463-1468. doi:10.1023/A:1011970125687
23. Karlsson MO, Savic RM. Diagnosing model diagnostics. *Clin Pharmacol Ther*. 2007;82(1):17-20. doi:10.1038/sj.clpt.6100241
24. Bergstrand M, Hooker AC, Wallin JE, Karlsson MO. Prediction-corrected visual predictive checks for diagnosing nonlinear mixed-effects models. *AAPS J*. 2011;13(2):143-151. doi:10.1208/s12248-011-9255-z
25. Dosne AG, Bergstrand M, Harling K, Karlsson MO. Improving the estimation of parameter uncertainty distributions in nonlinear mixed effects models using sampling importance resampling. *J Pharmacokinet Pharmacodyn*. 2016;43(6):583-596. doi:10.1007/s10928-016-9487-8
26. Conradie A, Serbina N, Auffarth E, Nedelman J, Lombardi A, Alliance TB. TBAJ-587 and ERA4TB: a productive clinical development partnership. In: *International Workshop on Clinical Pharmacology for TB Drugs*. TB Alliance; 2023.
27. Svensson EM, Dosne AG, Karlsson MO. Population pharmacokinetics of bedaquiline and metabolite M2 in patients with drug-resistant tuberculosis: the effect of time-varying weight and albumin. *CPT Pharmacometrics Syst Pharmacol*. 2016;5(12):682-691. doi:10.1002/psp4.12147
28. Keutzer L, Salehabad YA, Forsman LD, Simonsson USH. A modeling-based proposal for safe and efficacious reintroduction of bedaquiline after dose interruption: a population pharmacokinetics study. *CPT Pharmacometrics Syst Pharmacol*. 2022;11(5):628-639.
29. Beal SL, Sheiner LB, Boeckmann AJ, Bauer RJ. *NONMEM 7.3.0 Users Guides*. ICON Development Solutions; 1989.
30. Lindstrom MJ, Bates DM. Nonlinear mixed effects models for repeated measures data. *Biometrics*. 1990;46(3):673-687. doi:10.2307/2532087
31. Free Software Foundation Inc. *GCC (Version 14.2)*. GCC Team; 2024.
32. Karlsson M, Nordgren R. *Perl Speaks NONMEM (Version 5.3.1)*. Uppsala University; 2023.
33. R Core Team. *R: A Language and Environment for Statistical Computing (Version 4.1.2)*. R Foundation for Statistical Computing; 2021.
34. Wickham H, Averick M, Bryan J, et al. Welcome to the {tidyverse}. *J Open Source Softw*. 2019;4(43):1686. doi:10.21105/joss.01686
35. Soetaert K, Petzoldt T, Setzer RW. Solving differential equations in R: package desolve. *J Stat Softw*. 2010;33(9):1-25.
36. Jonsson EN, Karlsson MO. Xpose—an S-PLUS based population pharmacokinetic/pharmacodynamic model building aid for NONMEM. *Comput Methods Programs Biomed*. 1999;58(1):51-64. doi:10.1016/s0169-2607(98)00067-4
37. Keizer RJ, Karlsson MO, Hooker AC. Modeling and simulation workbench for NONMEM: tutorial on Pirana, PsN, and Xpose. *CPT Pharmacometrics Syst Pharmacol*. 2013;2(6):1-9. doi:10.1038/psp.2013.24
38. Alexander SPH, Kelly E, Mathie AA, et al. The concise guide to PHARMACOLOGY 2023/24: introduction and other protein targets. *Br J Pharmacol*. 2023;180(Suppl 2):S1-S22.
39. Mouton JW, Meletiadis J, Voss A, Turnidge J. Variation of MIC measurements: the contribution of strain and laboratory variability to measurement precision. *J Antimicrob Chemother*. 2018;73(9):2374-2379. doi:10.1093/jac/dky232
40. McLeay SC, Vis P, Heeswijk RPGV, Green B. Population pharmacokinetics of bedaquiline (TMC207), a novel antituberculosis drug. *Antimicrob Agents Chemother*. 2014;58(9):5315-5324. doi:10.1128/AAC.01418-13

SUPPORTING INFORMATION

Additional supporting information can be found online in the Supporting Information section at the end of this article.

How to cite this article: Leding AAM, Bruinenberg P, Conradie A, et al. Population pharmacokinetics of TBAJ-587 and its main metabolites—Evaluation of different loading dose strategies and early dose selection. *Br J Clin Pharmacol*. 2025; 1-11. doi:10.1002/bcp.70333